ANALYSIS OF LOW-TEMPERATURE ELECTRON TRANSPORT IN A COMPOSITE FILM OF REDUCED GRAPHENE OXIDE WITH MOLYBDENUM DISULFIDE

N.V. Kurnosov[1], A.M. Plokhotnichenko[1], V.A. Karachevtsev[1]

[1] *B. Verkin Institute for Low Temperature Physics and Engineering of the National Academy of Sciences of Ukraine.*
Nauky Ave., 47, Kharkiv-61103, Ukraine.
E-mail: nick.kurnosov@gmail.com

rGO-MoS_2 composite: preparation, SEM characterization, temperature dependence of the resistance

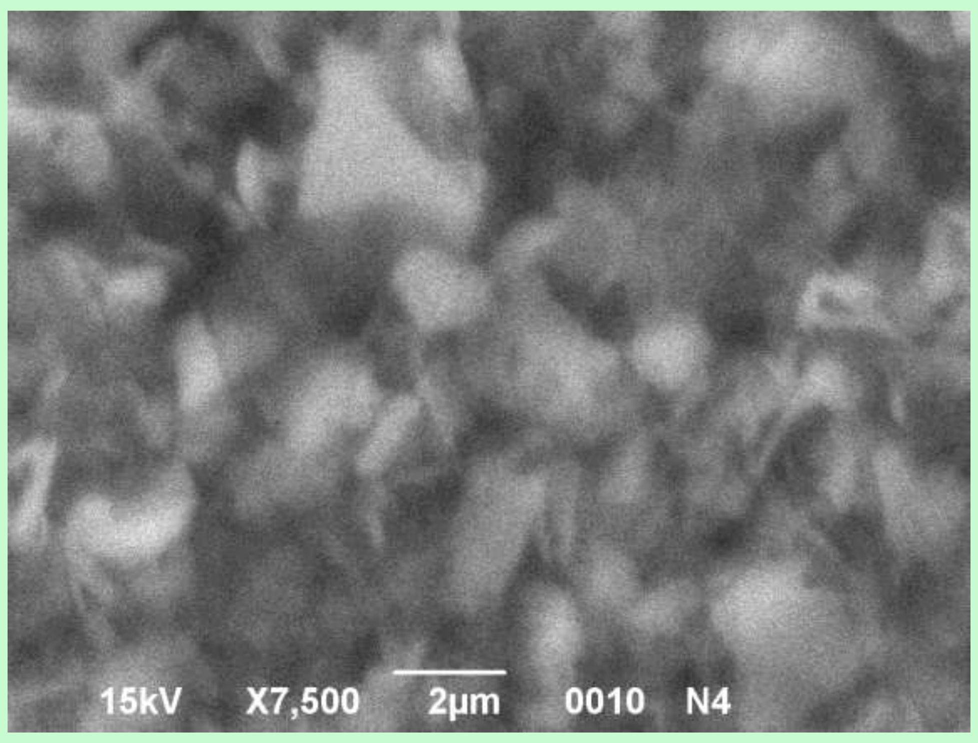

Fig. 1. SEM image of rGO-MoS_2 composite surface.

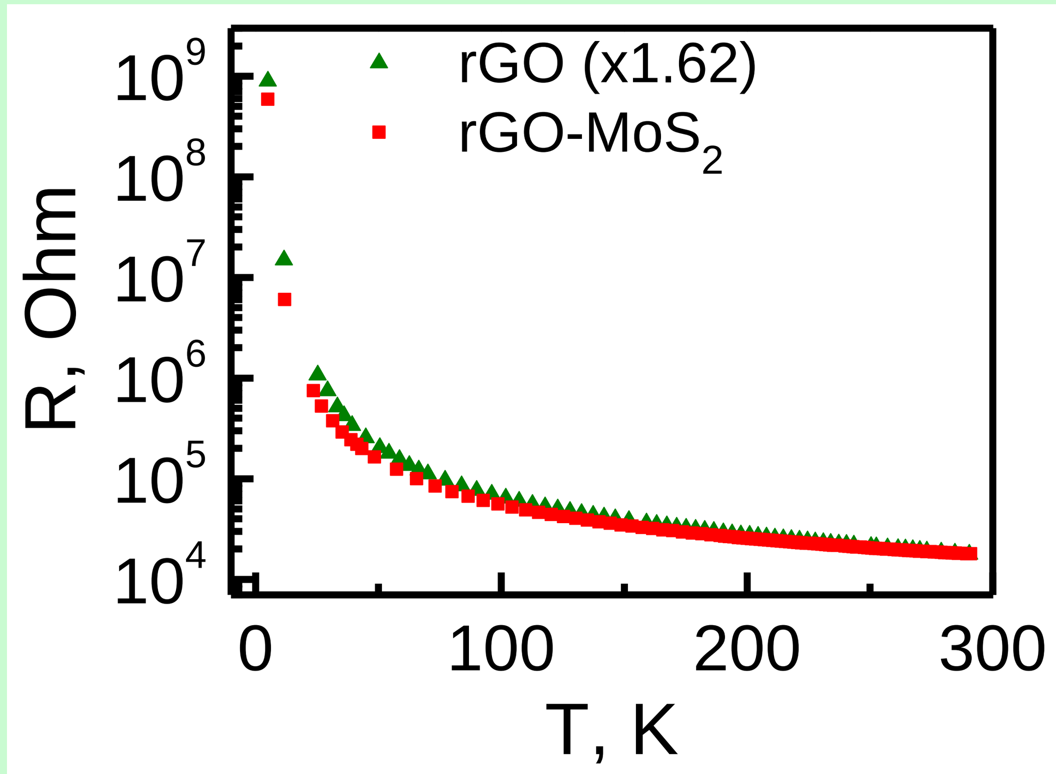

Fig. 2. Temperature dependence of the resistance (R(T)) of rGO-MoS_2 composite. R(T) of rGO film normalized to equal resistance at 290 K is also shown.

In our research we have studied composite containing **reduced graphene oxide (rGO)** and **molybdenum disulfide (MoS_2)**. MoS_2 (Sigma Aldrich) and rGO (Graphenea) were used as supplied. rGO had ~87% fraction of carbon which means large amount of conductive sp^2 domains . The **composite rGO-MoS_2 film** was obtained from suspension of rGO-MoS_2 hybrids in methanol deposited on the PTFE membrane (pores 0.24 μm) by vacuum filtration. Preparation of the suspension was based on ultrasound treatment (60 min, 22 kHz) with following centrifugation (3000g, 15 min) of rGO and MoS_2 with 1:2 weight ratio . The rGO-MoS_2 film was then separated from the membrane.

SEM image of the surface of rGO-MoS_2 composite is shown in Fig. 1. We assume that mainly MoS_2 flakes can be seen on the surface, the average size of these structures is several μm.

Resistance of rGO-MoS_2 composite film was measured in the temperature range of 5–290 K using gas-helium cryostat. R(T) dependence of rGO-MoS_2 composite is shown in Fig. 2 along with data obtained earlier for rGO film [1]. Given the large **relative increase of resistance at temperature decrease** (more than 4 orders of magnitude), we emphasize that the **R(T) dependences of rGO-MoS_2 and rGO samples are very similar in the whole temperature range measured**. Therefore, we assume that electron transport in rGO-MoS_2 composite is mainly determined by a **manifold of inherently conductive rGO nanosheets**.

Analysis of low-temperature electronic transport in rGO-MoS_2 and rGO. Efros-Shklovskii model

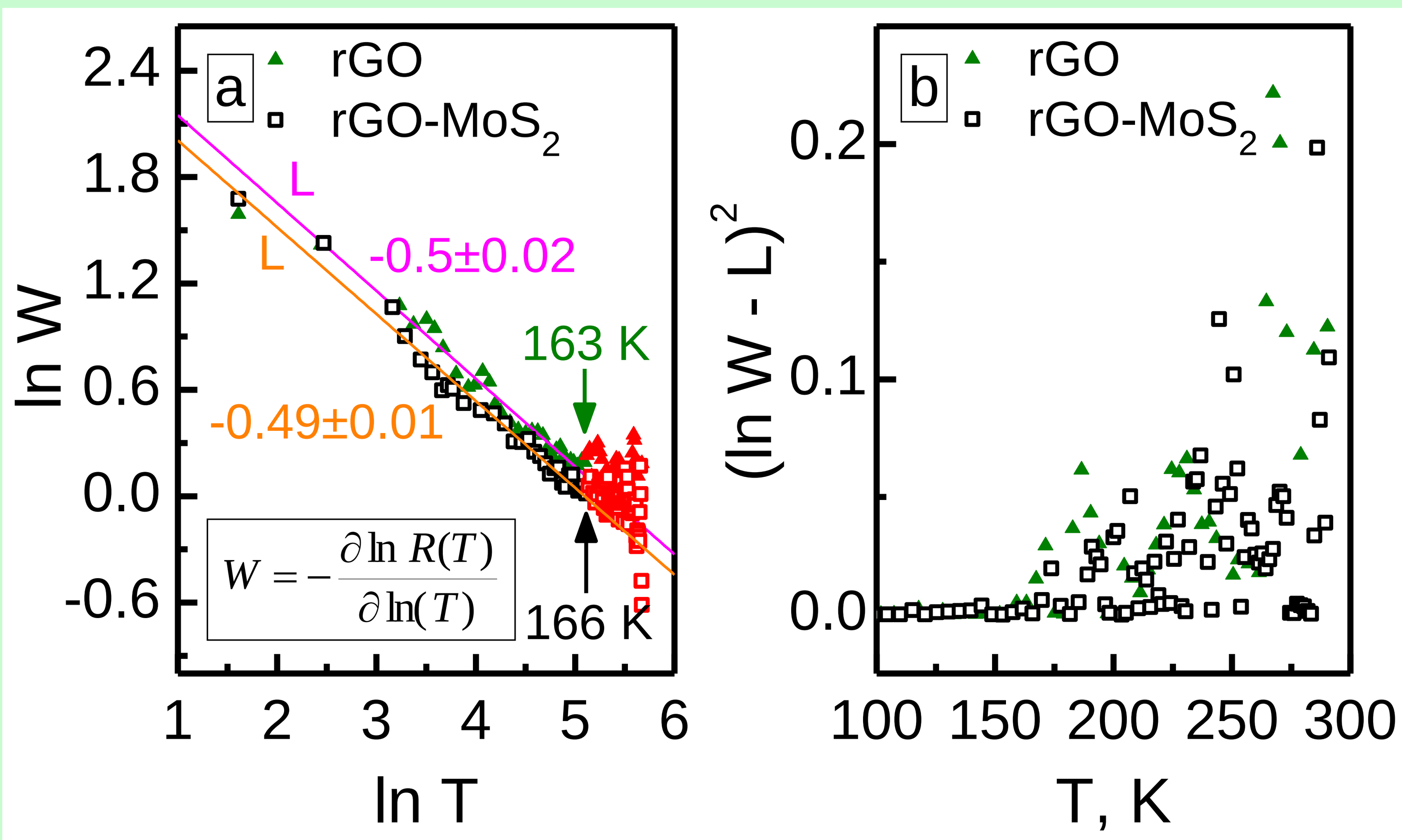

Fig. 3. a – Temperature dependences of reduced activation energy W calculated for the rGO-MoS_2 and rGO films (ln-ln plot). Linear fits (L) and resulting slopes are shown. Arrows indicate the high-temperature margins of linear fits.
b - quadratic deviation between ln(W) data points and linear fits.

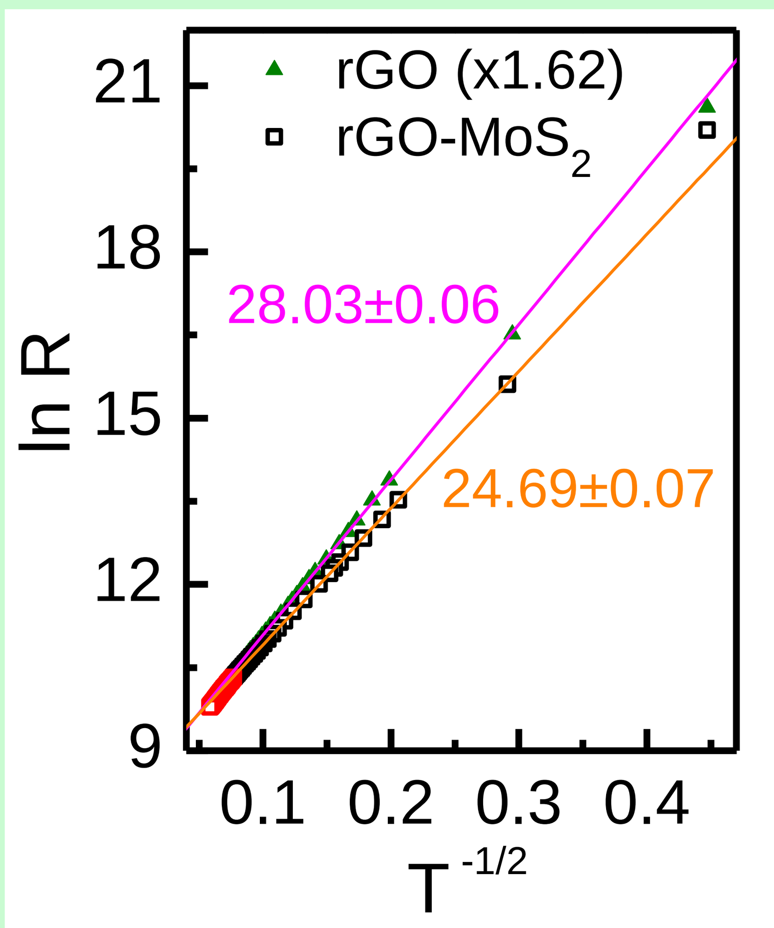

Fig. 4. Semilogarithmic plots of ln(R) vs $T^{-1/2}$ for the rGO-MoS_2 composite and rGO film. Slopes of linear fits are indicated.

Both films display semiconducting behaviour of R(T). We assume that electron transport at low temperatures is governed by variable-range hopping (VRH) which relies on phonon-assisted tunneling of electrons between localized states [2]. Within generalized VRH model **$R(T) \sim \exp[(T_0/T)^m]$, $0<m<1$**.

In order to confirm the applicability of VRH to our samples and precisely determine the exponent ***m*** we have calculated reduced activation energy W, plotted ln(W) vs ln(T) and performed linear fitting up to indicated temperatures, similarly to our earlier study [1]. The results are shown in Fig. 3a. Slopes are confirmed to be effectively equal and we get ***m*=1/2** for both rGO-MoS_2 and rGO samples. Therefore, the low-temperature conductivity in rGO-MoS_2 composite (as well as rGO film) is governed by the **Efros-Shklovskii mechanism (ES VRH)** which accounts for Coulomb gap phenomenon [3] and was observed earlier in graphene-related samples [4]. Fig. 3b presents quadratic deviations between ln(W) data points and respective fitted lines L in the temperature range of 100-290 K. At temperatures higher than 166 K (rGO-MoS_2) and 163 K (rGO) average data scattering of ln(W) is increased rather abruptly. We assume that **transition from ES VRH to another transport model** occurs at indicated temperatures. We also plotted R(T) dependences in ln(R) vs $T^{-1/2}$ coordinates, performed linear fits and obtained T_0 parameters, 610 and 786 K for rGO-MoS_2 and rGO (second powers of slopes in Fig. 4). **Coulomb gap widths** (directly proportional to T_0 [4]) were estimated as ~60 and 80 K.

Applicability of Mott VRH and power law models in higher-temperature range of R(T) dependences

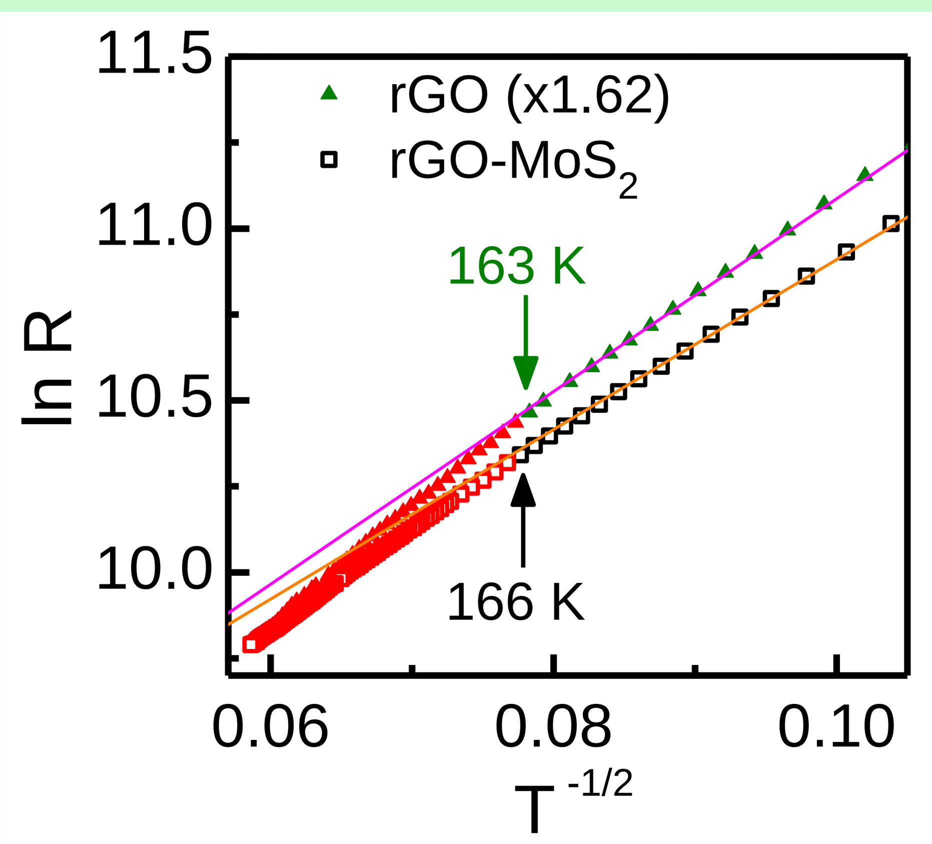

Fig. 5. Semilogarithmic plots of ln(R) vs $T^{-1/2}$ for the rGO-MoS_2 composite and rGO film in the higher-temperature range.

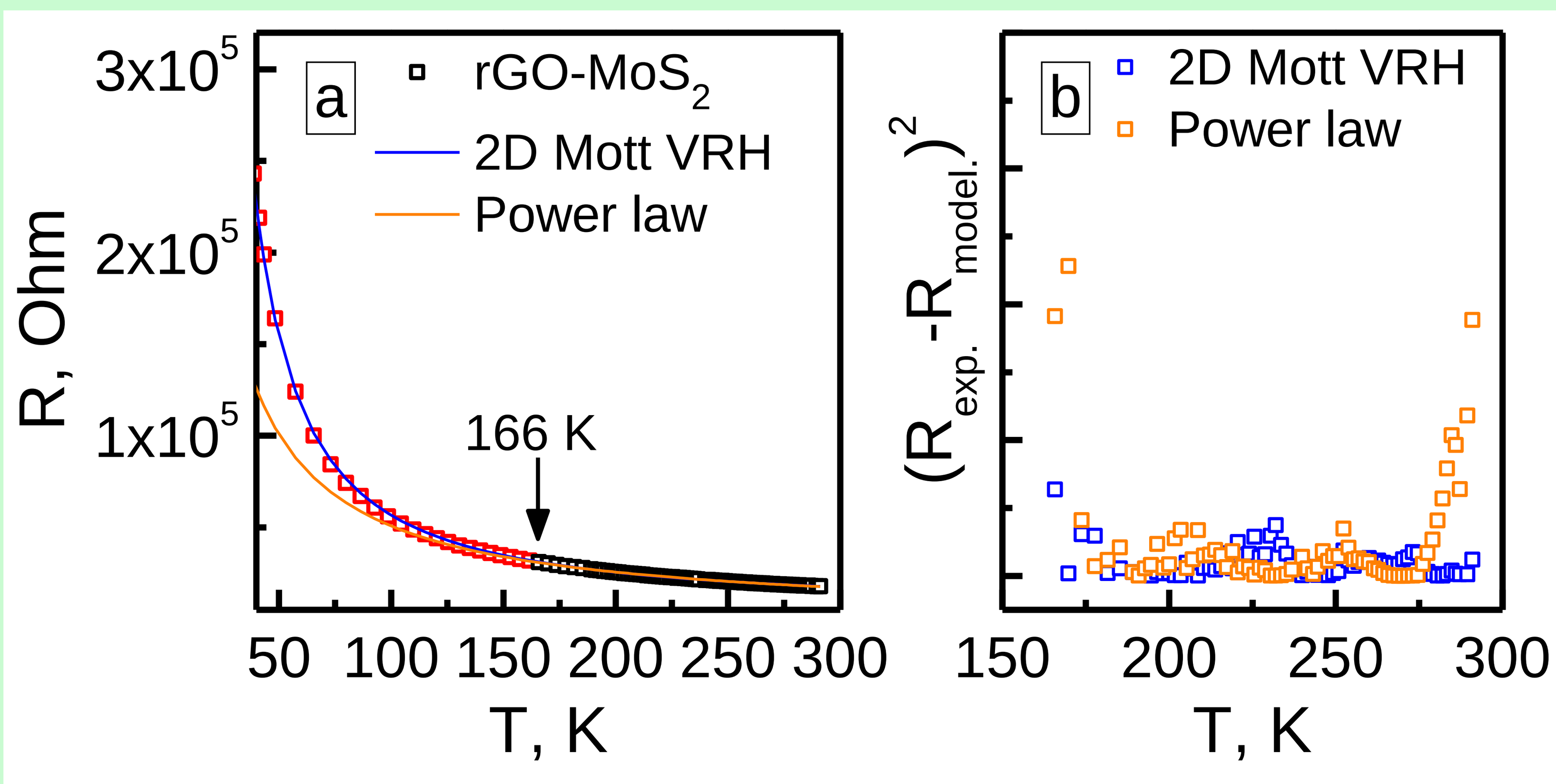

Fig. 6. a – R(T) dependence of rGO-MoS_2 composite, points marked black (T>166 K) were fitted with 2D Mott VRH and power law models. b – Squared residuals between experimental R(T) data points and calculated fitting curves.

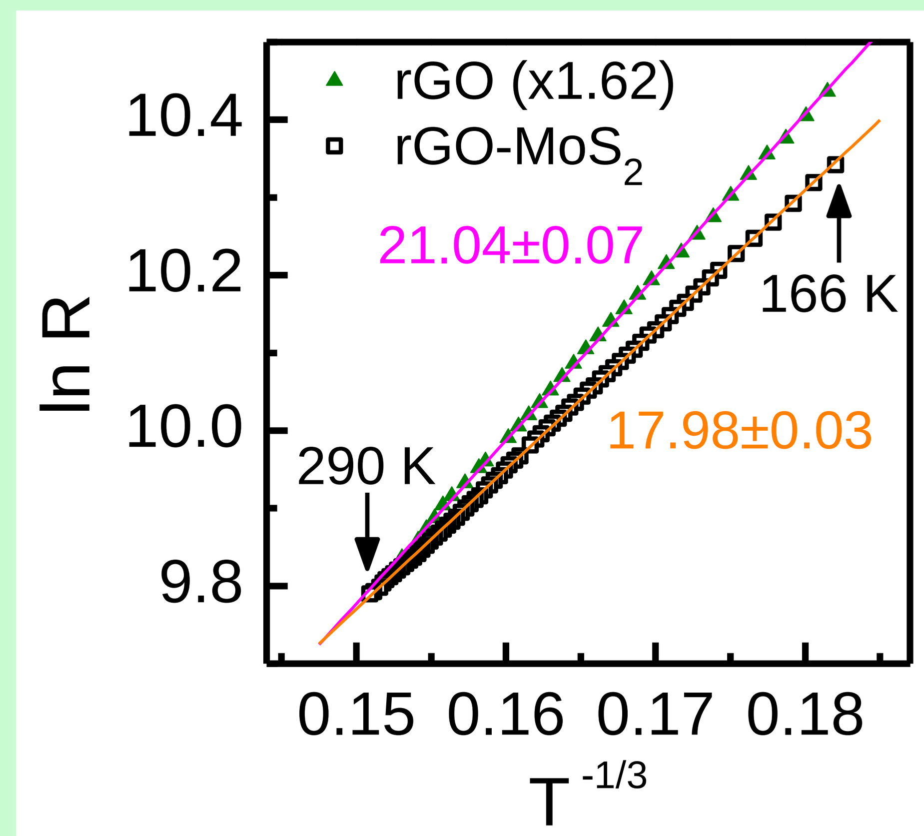

Fig. 7. Semilogarithmic plots (ln(R) vs $T^{-1/3}$) in higher-temperature range for the rGO-MoS_2 and rGO films. Slopes of linear fit are indicated.

As the ES VRH model is valid **specifically for the tunneling between localized states inside the Coulomb gap**, one can expect the deviation from ES VRH at a temperature increase. Note that data points **gradually decline** from corresponding linear fits in the high-temperature ranges of ln R vs $T^{-1/2}$ dependences plotted for rGO-MoS_2 and rGO samples (Fig. 5, red points). We have performed an approximation of higher-temperature ranges of experimental R(T) dependences using both **two-dimensional Mott VRH (2D Mott VRH)** $R(T) \sim \exp[(T_0/T)^{1/3}]$ and **power law** $R(T) \sim T^{-p}$ model (already used for study of electron transport in thin rGO devices [5]), the results are shown in Fig. 6a for the rGO-MoS_2 composite. A comparison of squared residuals (Fig. 6b) shows that in the specified temperature range (T > 166 K) the **2D Mott VRH model fits experimental data better**. In addition, while 2D Mott VRH was used for fitting to the R(T) dependence in the higher-temperature range, **the curve obtained also closely follows the R(T) dependence at lower temperatures** (T < 166 K) in contrast to the power law curve (Fig. 6a). Thus, we assume that the **crossover from ES VRH to 2D Mott VRH** occurs for our rGO-MoS_2 composite at a temperature increase similarly to rGO film [1]. According to the 2D Mott VRH model, the experimental R(T) dependences in the higher-temperature range can be plotted in ln(R) vs $T^{-1/3}$ coordinates and fitted linearly, the results are shown in Fig. 7. The characteristic T_0 temperatures (fourth powers of slopes in Fig. 7) are 5813 K and 9314 K for the rGO-MoS_2 and rGO, respectively. Also note that **2D Mott VRH regime persists up to room temperature**. The experimental results presented here have been published recently [6].

Conclusions

Electrical resistance of rGO-MoS_2 composite was measured in the wide temperature range of 5–290 K in order to study the electronic transport properties. The detailed analysis of resistance temperature dependence R(T) as well as comparison to rGO film has proved that at low temperatures (from 5 till ~166 K) the electronic transport in composite fully corresponds to Efros-Shklovskii variable-range hopping (ES VRH) which is a distinctive feature of disordered semiconductors with a Coulomb gap. At higher temperatures we have used Mott VRH and power law models for fitting of experimental R(T) and have confirmed a transition from ES VRH to 2D Mott VRH as the temperature becomes much larger than the estimated Coulomb gap width. Similarity in the behavior of R(T) dependences, applicability of the same transport models for rGO-MoS_2 and rGO samples indicate that electron transport in the composite is determined by the inherent conductivity of rGO nanosheets, however, we also find slight differences from rGO film in terms of transport parameters.

References

[1] N.V. Kurnosov, A.S. Linnik, V.A. Karachevtsev // Low Temp. Phys.-2020.-46.-P. 346.
[2] N.F. Mott and E.A. Davis, Electronic Processes in Non-Crystalline Materials, Oxford: Clarendon, 1979
[3] B.I. Shklovskii and A.L. Efros, Electronic Properties of Doped Semiconductors, Springer-Verlag, 1984
[4] M. Park, S.J. Hong, K.H. Kim, et. al. // Appl. Phys. Lett.-2017.-111.-P. 173103.
[5] A. Kovtun, A. Candini, A. Vianelli, et. al. // ACS Nano-2021.-15.-P. 2654.
[6] N.V. Kurnosov, A.M. Plokhotnichenko, V.A. Karachevtsev // Appl.Phys.A-2025.-131.-P. 190.